



**HAL**  
open science

## Structure, function, and evolution of Gga -AvBD11, the archetype of the structural avian-double- $\beta$ -defensin family

Nicolas Guyot, Herve Meudal, Sascha Trapp, Sophie Iochmann, Anne Silvestre, Guillaume Jousset, Valérie Labas, Pascale Reverdiau, Karine Loth, Virginie Herve, et al.

### ► To cite this version:

Nicolas Guyot, Herve Meudal, Sascha Trapp, Sophie Iochmann, Anne Silvestre, et al.. Structure, function, and evolution of Gga -AvBD11, the archetype of the structural avian-double- $\beta$ -defensin family. *Proceedings of the National Academy of Sciences of the United States of America*, 2020, 117 (1), pp.337-345. 10.1073/pnas.1912941117 . hal-02522250

**HAL Id: hal-02522250**

**<https://hal.science/hal-02522250v1>**

Submitted on 24 Nov 2020

**HAL** is a multi-disciplinary open access archive for the deposit and dissemination of scientific research documents, whether they are published or not. The documents may come from teaching and research institutions in France or abroad, or from public or private research centers.

L'archive ouverte pluridisciplinaire **HAL**, est destinée au dépôt et à la diffusion de documents scientifiques de niveau recherche, publiés ou non, émanant des établissements d'enseignement et de recherche français ou étrangers, des laboratoires publics ou privés.

# Structure, function and evolution of *Gga-AvBD11*, the archetype of a new structural avian-double- $\beta$ -defensin family

Nicolas Guyot<sup>1</sup>, Hervé Meudal<sup>2</sup>, Sascha Trapp<sup>3</sup>, Sophie lochmann<sup>4</sup>, Anne Silvestre<sup>3</sup>, Guillaume Jousset<sup>2</sup>, Valérie Labas<sup>5,6</sup>, Pascale Reverdiau<sup>4</sup>, Karine Loth<sup>2,7</sup>, Virginie Hervé<sup>4</sup>, Vincent Aucagne<sup>2</sup>, Agnès F. Delmas<sup>2</sup>, Sophie Rehault-Godbert<sup>1\*</sup>, Céline Landon<sup>2\*</sup>. Corresponding authors: [celine.landon@cnrs-orleans.fr](mailto:celine.landon@cnrs-orleans.fr); [sophie.rehault-godbert@inra.fr](mailto:sophie.rehault-godbert@inra.fr)

<sup>1</sup>BOA, INRA, Université de Tours, 37380, Nouzilly, France <sup>2</sup>CBM, CNRS, 45071, Orléans, France <sup>3</sup>ISP, INRA, Université de Tours, 37380, Nouzilly, France <sup>4</sup>CEPR, INSERM, Université de Tours, 37032, Tours, France <sup>5</sup>PRC, INRA, CNRS, IFCE, Université de Tours, 37380, Nouzilly, France <sup>6</sup>PAIB, CIRE, INRA, CHRU, Université de Tours, 37380, Nouzilly, France <sup>7</sup>UFR CoST, Université d'Orléans, 45100, Orléans, France

Submitted to Proceedings of the National Academy of Sciences of the United States of America

**Out of the 14 avian  $\beta$ -defensins identified in the *Gallus gallus* genome, only three are present in the chicken egg, including the egg-specific avian  $\beta$ -defensin 11 (*Gga-AvBD11*). Given its specific localization and its established antibacterial activity, *Gga-AvBD11* appears to play a protective role in embryonic development. *Gga-AvBD11* is an atypical double-sized defensin, predicted to possess two motifs related to  $\beta$ -defensins and six disulfide bridges. The 3D NMR structure of the purified *Gga-AvBD11* is a compact fold composed of two packed  $\beta$ -defensin domains. This fold is the archetype of a new structural family, dubbed herein as avian-double- $\beta$ -defensins (Av-DBD). We speculate that *AvBD11* emanated from a mono-domain gene ancestor and that similar events might have occurred in arthropods, leading to another structural family of less compact DBDs. We show that *Gga-AvBD11* displays antimicrobial activities against Gram+ and Gram- bacterial pathogens, the avian protozoan *Eimeria tenella* and avian influenza virus. *Gga-AvBD11* also shows cytotoxic and anti-invasive activities, suggesting that it may not only be involved in innate protection of the chicken embryo, but also in the (re-)modeling of embryonic tissues. Finally, the contribution of either of the two *Gga-AvBD11* domains to these biological activities was assessed, using chemically synthesized peptides. Our results point to a critical importance of the cationic N-ter domain in mediating antibacterial, antiparasitic and anti-invasive activities, with the C-ter domain potentiating the two latter activities. Strikingly, antiviral activity in infected chicken cells, accompanied by marked cytotoxicity, requires the full-length protein.**

defensins, avian-double- $\beta$ -defensin | avian egg, chicken | phylogeny, NMR structure | antimicrobial activities, *Eimeria*, avian influenza virus | immunomodulation, alarmins

## Introduction

Avian  $\beta$ -defensins 11 (AvBD11s) are atypical defensins found in birds that are essentially expressed in the oviduct (1). This localisation suggests physiological roles related to avian reproduction and/or to the development of the avian embryo. AvBD11 from *Gallus gallus* (*Gga-AvBD11*, aka VMO-2), which is also present in eggshell and in egg white, is one of the main components of the outer layer of hen egg vitelline membrane (VM) (2), the last protective barrier of the embryo (3-5). Consistent with its surmised role as an antimicrobial peptide, we have previously shown that purified *Gga-AvBD11* displays antibacterial activities against Gram-positive and Gram-negative bacteria (6, 7). Next to its contribution to the egg's innate immunity against pathogen infection, *Gga-AvBD11* may also regulate embryo growth and the expansion of extraembryonic membranes. The VM outer layer assists in the growth of the extra-embryonic vascularized yolk sac during embryogenesis, suggesting that *Gga-AvBD11* may also have a significant role in angiogenesis and cell migration.

The sequence of *Gga-AvBD11* contains two predicted  $\beta$ -defensin motifs (Fig. 1) (7) and represents the sole double-sized defensin (9.8 kDa) among all 14 AvBDs reported in the chicken species. Such atypical structural features raise questions regarding the independent or synergistic roles of the two predictive motifs. The presence of an AvBD11 protein was described in eggs of quail (8) and turkey (9), and similar sequences were also reported for the green lizard *Anolis carolinensis* (AcBD14 (10) and helofensin3-like protein (11)), and for the Komodo dragon (12) but not in other animal classes.

The benefit for the avian/reptile species of possessing a double-sized defensin is a fascinating question. The aim of the present work was to investigate the roles of *Gga-AvBD11* and of its two isolated predicted  $\beta$ -defensin motifs (Fig. 1). The resolution of the *Gga-AvBD11* structure by NMR revealed a new and compact 3D fold that we named avian-double- $\beta$ -defensin (Av-DBD). The three molecules (*Gga-AvBD11*, N-ter and C-ter peptides) were tested for antimicrobial activities, for their immunomodulatory properties and their effect on cell viability and cell invasion. Our results clearly demonstrate that: i) antibacterial effects are carried by the N-ter domain; ii) antiparasitic and anti-invasive activities are mainly mediated by the N-ter domain, but

## Significance

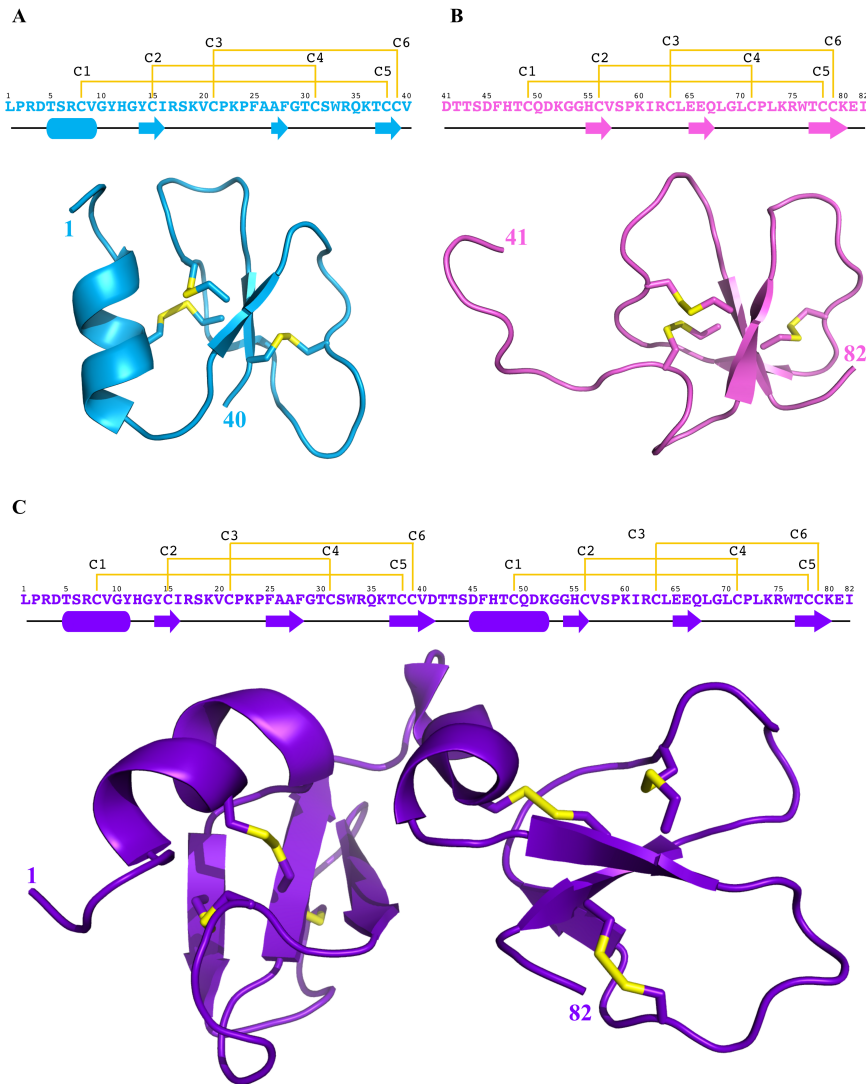
The 3D structure of *Gga-AvBD11* (*Gallus gallus* avian  $\beta$ -defensin-11) is characterized by two packed  $\beta$ -defensin domains. This makes *Gga-AvBD11* the type member of a new structural family dubbed avian-double- $\beta$ -defensin (Av-DBD). Its high sequence conservation among bird species suggests essential roles in the avian egg. Our results present *Gga-AvBD11* as an effector of innate immunity with a broad spectrum of activities against bacterial pathogens, *Eimeria* parasites and avian influenza virus. In addition, it seems to modulate cell viability, proliferation and invasiveness. Thus, *Gga-AvBD11* is likely to assist in the proper development and defense of the avian embryo. Antibacterial, antiparasitic and anti-invasive activities are mainly mediated by its N-terminal domain. Strikingly, antiviral activity requires the full-length protein at cytotoxic concentrations.

## Reserved for Publication Footnotes





273  
274  
275  
276  
277  
278  
279  
280  
281  
282  
283  
284  
285  
286  
287  
288  
289  
290  
291  
292  
293  
294  
295  
296  
297  
298  
299  
300  
301  
302  
303  
304  
305  
306  
307  
308  
309  
310  
311  
312  
313  
314  
315  
316  
317  
318  
319  
320  
321  
322  
323  
324  
325  
326  
327  
328  
329  
330  
331  
332  
333  
334  
335  
336  
337  
338  
339  
340



PDF

Fig. 3. Sequence, cysteines bonding pattern and 3D structure of A / N-ter peptide [1-40]*Gga*-AvBD11 in cyan, B / C-ter peptide [41-82]*Gga*-AvBD11 in pink, and C / the full-length [1-82]*Gga*-AvBD11 in purple. Disulfide bridges are shown in yellow. Drawn with PYMOL (55)

*AvBD11* gene was found in 69 avian species, which cover 32 orders out of the 40 orders of birds. The resulting AvBD11 proteins share high sequence identity with *Gga*-AvBD11 (Fig. 2). The strict conservation of the position of the 12 Cys residues suggests that the 3D structure of *Gga*-AvBD11 constitutes a structural archetype for all AvBD11s.

**AvBD11 sequence contains two motifs related to  $\beta$ -defensins, with different physico-chemical properties**

In vertebrates, the two main groups of defensins,  $\alpha$ - and  $\beta$ -defensins, differ in their disulfide pairing and the inter-cysteine spacing (13). In birds, only  $\beta$ -defensins have been identified (14). Mature *Gga*-AvBD11 is a cationic peptide (theoretical pI: 8.8) of 82 amino acids containing 12 cysteines involved in six disulfide bonds (7). The number of cysteines and the spacing between cysteines (CX<sub>6</sub>CX<sub>5</sub>CX<sub>9</sub>CX<sub>6</sub>CC and CX<sub>6</sub>CX<sub>6</sub>CX<sub>7</sub>CX<sub>6</sub>CC) led us to predict the presence of two  $\beta$ -defensins-related motifs, corresponding to exon 2 and 3, respectively (Fig. 1). Consistent with this, mass spectrometry fragmentation profile analysis readily revealed two fragmentation-resistant regions separated by a central fragmentation-sensitive area (SI Appendix, S1-S4). Using bioinformatics tools, we analyzed charge and hydrophobicity of each defined moiety: [1-40]*Gga*-AvBD11 is clearly cationic, while [41-82]*Gga*-AvBD11 is rather neutral (theoretical pI: 9.3 vs. 6.9;

total net charge: +6 vs. 0, respectively). In addition, the C-ter domain is more hydrophilic than the N-ter domain.

***Gga*-AvBD11 structure is the archetype of avian- double- $\beta$ -defensins**

We determined by NMR the 3D structures of the entire protein [1-82]*Gga*-AvBD11 purified from hen eggs as well as the two peptide domains [1-40]*Gga*-AvBD11 and [41-82]*Gga*-AvBD11. The two peptides were produced by solid phase peptide synthesis and oxidative folding under optimized conditions (SI Appendix, S5-S15). Their 3D structures were calculated by taking into account the restraints summarized in (SI Appendix, S16-S18). Both N-ter and C-ter peptides fold into a typical  $\beta$ -defensin motif: a three stranded antiparallel  $\beta$ -sheet (residues 14-16, 27-28, 37-39 and 55-57, 65-67, 77-80, respectively) stabilized by a C1-C5, C2-C4, C3-C6 disulfide bridges array (Fig. 3A and B). [1-40]*Gga*-AvBD11 displays a short  $\alpha$ -helix in its N-terminal part (residues 5-9). The 3D structure of the full-length protein reveals the presence of two  $\beta$ -defensin domains (Fig. 3C), with  $\beta$ 2 and  $\beta$ 3-strands slightly longer than in the N-ter peptide ( $\beta$ 2:25-28,  $\beta$ 3:37-41). The first helix is longer than in the N-ter peptide, and residues 45-52 that are unstructured in the C-ter peptide, form a second warped helix composed of a  $3_{10}$  helix turn (residues 45-48) followed by an  $\alpha$ -helix turn (residues 49-52). Hydrophobic interactions involving Ala26, Phe28, Val40, Phe46, Gln67 and

341  
342  
343  
344  
345  
346  
347  
348  
349  
350  
351  
352  
353  
354  
355  
356  
357  
358  
359  
360  
361  
362  
363  
364  
365  
366  
367  
368  
369  
370  
371  
372  
373  
374  
375  
376  
377  
378  
379  
380  
381  
382  
383  
384  
385  
386  
387  
388  
389  
390  
391  
392  
393  
394  
395  
396  
397  
398  
399  
400  
401  
402  
403  
404  
405  
406  
407  
408



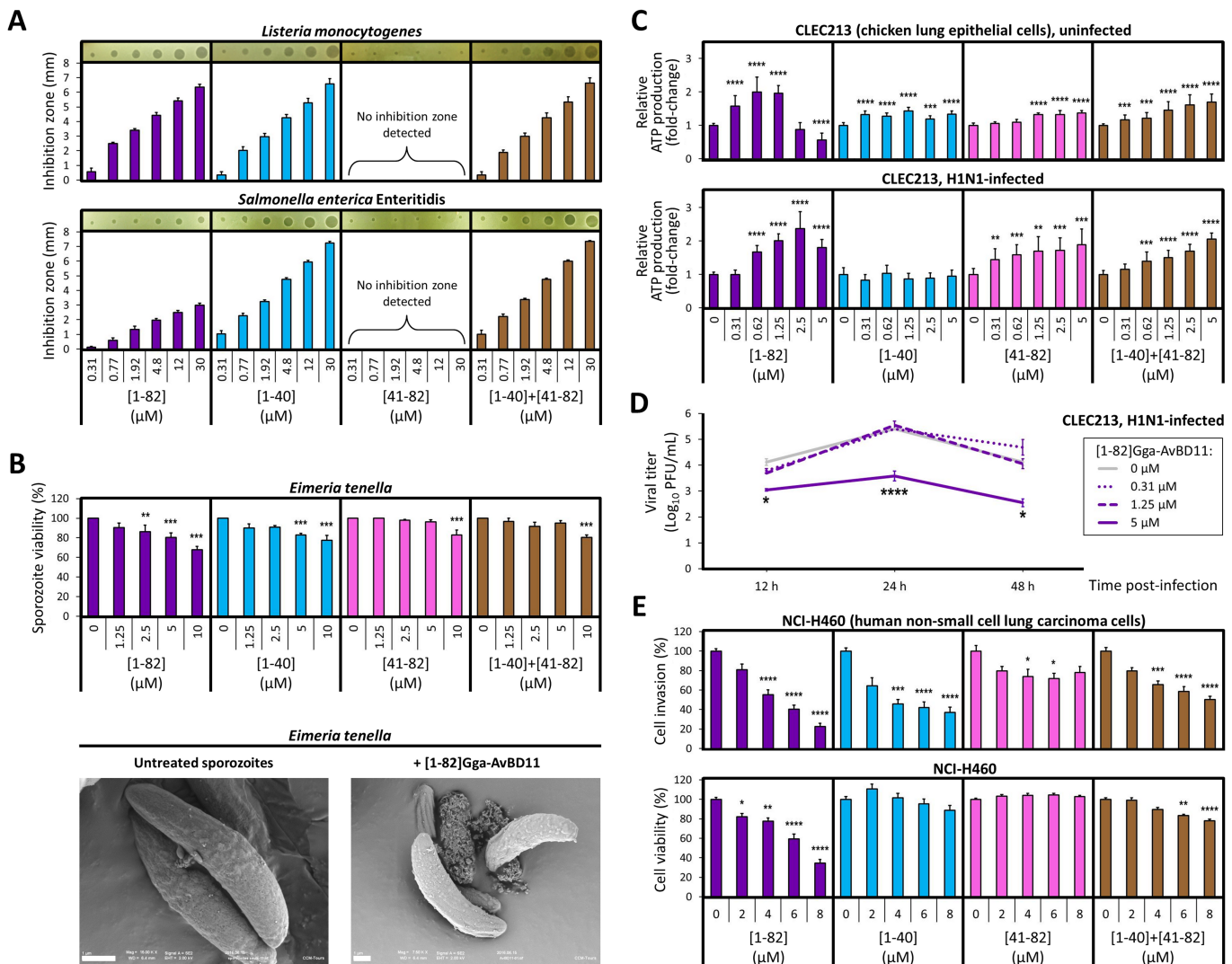


**Fig. 4. Functional characterization of *Gga-AvBD11* ([1-82]), its derived N-ter ([1-40]) and C-ter ([41-82]) peptides, and the combination [1-40]+[41-82]. (A)** Antibacterial activities against *L. monocytogenes* and *S. enterica* Enteritidis. Inhibition zones were shown as a function of molecule concentrations. Data are presented as means  $\pm$  SEM of at least 4 independent experiments performed in duplicates. Representative pictures of inhibition zones are shown in insets. (B) Antiparasitic activities against *E. tenella* sporozoites. Top panel: data represent means  $\pm$  SEM of sporozoite viability for at least 3 independent experiments performed in duplicates. Bottom panel: scanning electron microscopy analysis of *E. tenella* sporozoites under control conditions or treated with *Gga-AvBD11*. The scale bar represents 1  $\mu\text{m}$ . (C) Relative ATP production as a measure for treatment/virus-induced cytotoxic or cytopathogenic effects in non-infected or H1N1 virus-infected CLEC213. Relative ATP production rates for treated and/or infected cells were calculated as fold-changes with reference to mean control values (non-treated cells) set to 1. Shown are means  $\pm$  SEM from min. 2 independent experiments with 6 replicate samples. (D) H1N1 growth kinetics in *Gga-AvBD11*-treated CLEC213. CLEC213 were infected at an MOI 0.01 and viral titers (PFU/mL) in cell culture supernatants at 12 h, 24 h and 48 h post infection (pi) were determined by conventional plaque assay on MDBK cells. Shown are means  $\pm$  SEM from 1 experiment with duplicate samples. (E) Effects on invasion and viability of the human non-small cell lung cancer cell line NCI-H460. Data are presented as the percentage of invasive cells or cell viability compared to those of control cells without any molecule added. Results were expressed as means  $\pm$  SEM of at least 5 independent experiments performed at least in duplicates. (B), (C), (D), (E) Statistical significance: \*  $p < 0.05$ ; \*\*  $p < 0.01$ ; \*\*\*  $p < 0.001$ ; \*\*\*\*  $p < 0.0001$ .

Leu68 stabilize a compact 3D fold (SI Appendix, S19). The NMR titration of the N-ter peptide with the C-ter peptide (SI Appendix, S20) does not indicate any interaction between the domains, which suggests an essential role of the covalent link between the two domains in the full-length protein.

**The antibacterial activities of *Gga-AvBD11* against *Listeria monocytogenes* and *Salmonella* Enteritidis is mediated by the N-ter domain**

Antibacterial activities were tested against *Listeria monocytogenes* (Gram+) and *Salmonella* Enteritidis (Gram-), two bacterial pathogens responsible for food poisoning. The N-ter peptide was active against both bacteria with minimal inhibition concentration values (0.14  $\mu\text{M}$  and 0.31  $\mu\text{M}$ , respectively) in the same range to those obtained with the entire *Gga-AvBD11* (0.21  $\mu\text{M}$  and

0.15  $\mu\text{M}$ , respectively) (Fig. 4A, and S21). In contrast, the C-ter peptide showed no detectable activity against the two bacteria. Neither potentiation nor inhibition of the overall activity was observed when both peptides were used in combination. Altogether, these results suggest that the antibacterial activity of *Gga-AvBD11* is carried by the cationic N-ter region.

**Antiparasitic activity against *Eimeria tenella* sporozoites is mediated by the N-ter peptide, but most pronounced for the full length *Gga-AvBD11***

Antiparasitic activity was determined by using cell-free test inhibition assay on the infectious sporozoite forms of the protozoan *Eimeria tenella*, the causative agent of cecal avian coccidiosis (15). *Gga-AvBD11* showed a stronger antiparasitic activity than the N-ter peptide alone, which suggests amplification of the effect of

the N-ter domain by the C-ter domain in the full-length molecule (Fig. 4B). However, the C-ter peptide proved to be inactive, except at the highest dose tested (10  $\mu$ M), and neither synergy nor antagonism was observed when both peptides were used in combination. Sporozoites were further examined by scanning electron microscopy. Upon treatment with *Gga*-AvBD11, they underwent distinct structural alterations (Fig. 4B and SI Appendix, S22).

#### ***Gga*-AvBD11 displays net antiviral activity at concentrations entailing cytotoxicity**

Cytotoxic and antiviral activities were tested in a chicken lung epithelial cell (CLEC213) model using the commercial Viral ToxGlo™ assay (Fig. 4C). *Gga*-AvBD11 at 0.31-1.25  $\mu$ M caused a significant increase in relative ATP production (as a measure for cell viability), while higher concentrations caused a modest (2.5  $\mu$ M) or marked decrease (5  $\mu$ M) in relative ATP production rates in non-infected cells. Consistently, treatment with 5.0  $\mu$ M *Gga*-AvBD11 led to distinct morphological changes (cell shrinkage, rounded cell shape) and a dramatic loss of viable cells in the treated CLEC213 cultures (SI Appendix, S23). Similar to full-length *Gga*-AvBD11 at concentrations  $\leq$  1.25  $\mu$ M, the N-ter and C-ter peptides (alone or in combination) caused a significant increase in relative ATP production in non-infected cells. However, unlike for *Gga*-AvBD11, no cytotoxicity was detected for the peptides. Antiviral activity was determined by assessing relative ATP production in CLEC213 infected with a cytopathic H1N1 avian influenza virus. *Gga*-AvBD11 treatment of infected cells resulted in a marked increase in relative ATP production rates, thus pointing to antiviral activity. At concentrations  $\leq$  1.25  $\mu$ M, this increase was paralleled by a significant increase in relative ATP production in the non-infected cells (see above), indicating that the antiviral effects at these concentrations are probably delusive and rather related to pro-proliferative activities of *Gga*-AvBD11. However, at concentrations of 2.5  $\mu$ M and 5.0  $\mu$ M, relative ATP production in virus-infected cells remained on an elevated level (2.4- and 1.8-fold increase), indicating that the cytotoxic activity of *Gga*-AvBD11 at concentrations  $\geq$  2.5  $\mu$ M is accompanied by net antiviral activity (outbalancing its cytotoxic effects). For the N-ter and C-ter peptides (alone or in combination), no such net antiviral activity was observed: significantly increased relative ATP production rates in virus-infected cells were paralleled by similar increases in the non-infected cells, pointing to pro-proliferative activities of the peptides in infected/non-infected cells as postulated for *Gga*-AvBD11 at concentrations  $\leq$  1.25  $\mu$ M.

Finally, dose-dependent antiviral activity of the full-length protein was confirmed by determining the growth kinetics of the H1N1 virus in *Gga*-AvBD11-treated CLEC213 (Fig. 4D). While treatments with 0.31  $\mu$ M and 1.25  $\mu$ M had virtually no effect on viral replication, treatment with 5  $\mu$ M *Gga*-AvBD11 led to a substantial reduction of viral titers at 12 h (12-fold), 24 h (59-fold) and 48 h (37-fold) post infection (pi).

#### ***Gga*-AvBD11 and its N-ter and C-ter peptides affect cell viability and invasion**

To explore the potential role of *Gga*-AvBD11 in regulating embryonic development and the expansion of the yolk sac membrane, we used NCI-H460 human cells derived from a human non-small cell lung carcinoma. The use of this human cell line is motivated by the very limited availability of chicken cell lines with high proliferative and invasive capacities, and by the fact that the NCI-H460 cell line exhibiting high invasive capacities and an epithelial-like morphology is commonly used to assess pro- and anti-invasive agents *in vitro* (16, 17). The data from these assays are shown in Fig. 4E. Upon treatment of NCI-H460 cells with *Gga*-AvBD11, the number of cancer cells invading and passing through Matrigel™ significantly decreased at concentrations  $\geq$  4  $\mu$ M. *Gga*-AvBD11 treatment also resulted in a dose-dependent, significant diminishment of cell viability. Still, at 4, 6 and 8  $\mu$ M, the *Gga*-AvBD11 effect on invasiveness was even more dramatic,

suggesting that this anti-invasive activity of *Gga*-AvBD11 is not solely linked to its action on cell viability. Treatment with the N-ter peptide induced a significant decrease in cell invasion  $\geq$  2  $\mu$ M without affecting cell viability. The C-ter peptide exhibited no cytotoxicity and had only a modest effect on invasion. When the cells were treated with the two peptides in combination, distinct anti-invasive and cytotoxic activities were detected, but to a lesser extent than for *Gga*-AvBD11.

#### ***Gga*-AvBD11 and its derivate peptides lack pro-inflammatory effects**

Using the transformed human bronchial epithelial cell line, BEAS-2B (CRL-9609) as a model, we explored pro-inflammatory treatment effects (SI Appendix, S25) by measuring interleukin-6 and -8 production in culture supernatants. We concluded that *Gga*-AvBD11, N-ter and C-ter peptides lack pro-inflammatory properties in this particular cell model. It should be highlighted that a significant cytotoxic effect of *Gga*-AvBD11 was observed at the highest concentration tested (10  $\mu$ M).

#### **Discussion**

The presence of an AvBD11 protein is predicted from the vast majority of avian genomes (18). Strikingly, however, neither a specific function nor a structural characterization of this protein has been established so far. Here, we focused on *Gga*-AvBD11 from *Gallus gallus*, as the archetype of a new structural family. We propose to dub this family "avian-double- $\beta$ -defensin" (Av-DBD), as we demonstrated that its compact fold is composed of two packed  $\beta$ -defensin domains (Fig.3C and SI Appendix, S19). Indeed, the 3D structure of *Gga*-AvBD11 reported here exhibits two  $\beta$ -defensin domains, even though the inter-cysteine spacing is not canonical for the C-ter domain[1].

Isolated N- and C-ter peptides display the typical 3-stranded antiparallel  $\beta$ -sheet of  $\beta$ -defensins (SI Appendix, S26), and their global fold are not drastically changed in the full-length protein (SI Appendix, S27), except for a slight lengthening of  $\beta$ 2- and  $\beta$ 3-strands and an additional helix at the beginning of the C-ter domain. The domains are packed together by a hydrophobic cluster leading to a compact structure (SI Appendix, S19). The residues involved in the cluster are highly conserved within the AvBD11 family (SI Appendix, S28). Phe28 constitutes the core of the cluster and is strictly unchanged. The surface of *Gga*-AvBD11 is globally positive. However, the C-ter domain exhibits a continuous negative area facing the cationic N-ter domain (SI Appendix, S29). This area involves residues globally conserved in the other AvBD11 sequences currently available (SI Appendix, S30). These preservation of hydrophobic and charged residues, in addition to the strict conservation of the position of Cys residues and the high degree of sequence identity in AvBD11s (Fig. 2), suggests that the 3D organization of *Gga*-AvBD11 is conserved in all birds. It should be mentioned that, to date, there is no reference for such a double- $\beta$ -defensin in all structural databanks (SI Appendix, S31). It is noteworthy that other double-domain disulfide-rich proteins, e.g. double inhibitor cystine knot peptides (ICK) (22), are reported in the literature, yet with differences in the position of Cys residues, the disulfide pairing and the 3D structure.

[1] Depending on the cysteine spacing and the more or less lack of structural elements, several terms emerge over the years to describe the different members of the enlarged  $\beta$ -defensin family: "defensin-like"19. Torres AM, et al. (2000) Defensin-like peptide-2 from platypus venom: member of a class of peptides with a distinct structural fold. *The Biochemical journal* 348 Pt 3:649-656., "defensin-related"20. Fox NK, Brenner SE, & Chandonia JM (2014) SCOPe: Structural Classification of Proteins—extended, integrating SCOP and ASTRAL data and classification of new structures. *Nucleic acids research* 42(Database issue):D304-309., and even recently "intermediate defensin-like"21. Torres AM, et al. (2014) Structure and antimicrobial activity of platypus 'intermediate' defensin-like peptide. *FEBS letters* 588(9):1821-1826.. However, no term has yet been widely accepted and we prefer here to use the generic term " $\beta$ -defensin".

To explore which biological functions could be exerted by each domain of *Gga*-AvBD11, we scanned the Protein Data Bank for structural homologs. As expected, the N-ter domain (as part of the full-length-protein or isolated peptide) fits with a large set of  $\beta$ -defensins, some  $\alpha$ -defensins and snake crotoamine. In contrast, the 3D structure of the C-ter peptide only matches platypus defensins, mouse mBD7 and crotoamine. More surprisingly, it displays structural homologies with the C-ter domain of tick carboxypeptidase inhibitor (TCI) (SI Appendix, S32). Even if the two domains of the TCI structure (2k2x.pdb) both resemble  $\beta$ -defensin domains (23), the flexible linker between the two globular domains prevents DALI software (24) to ascertain any structural homologies with the compact 3D structure of the full-length *Gga*-AvBD11. Although the flexibility of this linker was reported to be important for the recognition mechanism and further interaction with carboxypeptidase A (25), *Gga*-AvBD11's potential inhibitory activity against carboxypeptidase A was explored. Our results did not corroborate such an activity (SI Appendix, S33).

In order to identify other potential double- $\beta$ -defensins (DBD) - compact or not - in others species than birds, we extensively screened the sequence homologies related to *Gga*-AvBD11. We extracted a series of sequences from all branches of arthropods with the cysteine pattern of  $\beta$ -defensins (SI Appendix, S34), which led us to postulate a global organization into two  $\beta$ -defensin domains. However, the sequence identities with *Gga*-AvBD11 are drastically reduced (< 34%) compared to bird sequences, and none of the residues involved in the packing of *Gga*-AvBD11 (SI Appendix, S19) is conserved in arthropods. This feature suggests a less compact structure (as in TCI) or at least a different packing between the two presumed  $\beta$ -defensin domains that could be predictive of divergent biological properties.

Our unsuccessful attempts to identify sequences similar to *Gga*-AvBD11 in vertebrates other than reptiles raise questions about the appearance of this family during evolution. It is now well accepted that i) mono-domain  $\beta$ -defensins found in vertebrates emerged from an ancestral cephalochordate big-defensin (26); ii)  $\alpha$ -defensins, only found in mammals, are derived from  $\beta$ -defensins (26), and iii) cyclic  $\theta$ -defensins, a restricted class uniquely found in old-world monkeys, are derived from  $\alpha$ -defensins (27). Our current hypothesis predicts that *AvBD11* originates from the duplication and fusion of an ancestral mono-domain  $\beta$ -defensin gene, similar to what is reported for *Gila* monster helofensins (11). Because all our attempts to identify sequences related to double- $\beta$ -defensins in other vertebrates than reptiles (mammals, fishes, amphibians), we cannot presume the existence of an ancestor gene, common to birds and arthropods. Probably, an independent duplication-fusion event might have occurred during the evolution of arthropods.

Genomic plasticity of defensin-encoding sequences is known to foster the adaptability of the innate immune system and to enable the acquisition of new functions, as exemplified by  $\beta$ -defensins of venomous vertebrates, which have evolved to target ion channels of their preys (28). In birds, 12 new AvBDs have been acquired through duplication events among galliform and passeriform birds (29). *AvBD11* appeared in birds before the galliform-passeriform split that occurred around 100 million years ago (29), likely before the Paleognathae-Neognathae split (*AvBD11* in ratite species) and it is highly conserved in the avian genomes currently available (Fig 2.). The analysis of previously published phylogenetic trees (18, 30) suggests that AvBD11 might have diverged from AvBD10. The appearance of such a double-domain protein during evolution could be driven either by its increased biological potency compared to a single domain molecule, and/or by the necessity to acquire new functions carried only by the full-length protein. Because of the high concentration of *Gga*-AvBD11 in the vitelline membrane known to protect the embryo

and to support the growth of the extra-embryonic yolk sac, we assessed the antimicrobial activity of purified *Gga*-AvBD11 against various microbial pathogens and explored its biological effect on cell viability and invasion.

The two pathogenic bacteria *Listeria monocytogenes* and *Salmonella enterica* were previously reported to be sensitive to *Gga*-AvBD11 (6, 7). Our present results clearly show that this antimicrobial activity is carried by the cationic N-ter domain. Cationicity is considered as one of the most critical determinants for antibacterial activities, triggering electrostatic interactions of peptides with the negatively charged membranes of bacteria (31). Hydrophobicity is also an essential parameter as it governs the peptide insertion into the lipid bilayer. The N-ter peptide respects these two key features, its cationic properties being shared by most AvBD11s, whereas the C-ter domain, less hydrophobic, exhibits variable charge properties (SI Appendix, S30). Consequently, the addition of C-ter domain does not substantially affect the antibacterial potency of the N-ter domain (Fig. 4A and SI Appendix, S21).

Antiparasitic activities have been previously reported for other antimicrobial peptides such as cecropin, melittin, dermaseptin and cathelicidins (32, 33) and human  $\alpha$ -defensins (34-36). The present work extends this activity to the  $\beta$ -defensin family. We demonstrated that *Gga*-AvBD11 and, to a lesser extent, also the N-ter peptide exhibit antiparasitic activities against infectious sporozoites of *Eimeria tenella*, one of the three main *Eimeria* species responsible for avian coccidiosis (15). The exact mechanisms by which *Gga*-AvBD11 exerts its antiparasitic effects (aggregation (36), pore formation (35)) remains to be elucidated. However, it can be speculated that i) the high cationicity of the full-length *Gga*-AvBD11 and the N-ter peptide might be crucial to trigger the first peptide/membrane interaction and that ii) the C-ter domain might increase the anti-*Eimeria* effect of the N-ter domain.

Testing of the cytotoxic and antiviral activities of *Gga*-AvBD11 and its N-ter and/or C-ter peptides in the CLEC213 infection model revealed that *Gga*-AvBD11 displays net antiviral (anti-influenza) activity at concentrations that are cytotoxic in non-infected cells. Antiviral activity against Newcastle disease virus, an avian respiratory pathogen, has previously been reported for AvBD2 (37). However, to our knowledge, this is the first report of an avian  $\beta$ -defensin displaying antiviral activity against an avian influenza virus. Strikingly, the concomitant cytotoxic and antiviral activities were only seen for the full-length molecule and not for the N-ter and C-ter peptides (alone or in combination). Distinct antiviral mechanisms have been shown for human  $\alpha$ ,  $\beta$ , and  $\theta$  defensins (38): virus neutralization through binding to viral envelope/capsid proteins or cellular cognate receptors; inhibition of viral fusion and post-entry steps; and immunomodulatory activity. It is thus conceivable that the H1N1 virus inhibitory activity of *Gga*-AvBD11 may involve its binding to the viral hemagglutinin and/or neuraminidase glycoproteins, the viral entry receptor or an innate immune receptor. One might speculate that *Gga*-AvBD11 binding to negatively charged  $\alpha$ 2,3 galactose-linked sialic acid moieties, the principal hemagglutinin receptor for avian influenza viruses, may restrict H1N1 virus infection by impeding viral adsorption and entry into CLEC213 cells. However, in this case, one would expect that the cationic N-ter peptide would display similar antiviral activity as the full-length molecule, which is clearly not the case—at least not in our experimental conditions. We hypothesize that the cytotoxic and antiviral activities of *Gga*-AvBD11 are mediated by its binding to a yet unidentified innate immune receptor, thereby leading to the activation of coalescing antiviral and pro-apoptotic signaling pathways. This notion is supported by our observation that 5  $\mu$ M *Gga*-AvBD11 is a potent inducer of NF- $\kappa$ B activity in the HD11 chicken macrophage cell line (SI Appendix, S24). Interestingly, the proposed antiviral mechanism



817 is in good agreement with a previous report describing AvBD13  
818 as an activator of TLR4-mediated NF- $\kappa$ B signaling (39) and the  
819 concept of antimicrobial peptides serving as alarmins (40). Yet,  
820 it seems that the NF- $\kappa$ B-triggering activity of *Gga-AvBD11* is  
821 restricted to the chicken (and potentially other avian/sauropsid  
822 species), as no such activity could be detected in the human cell  
823 lines used in this study.

824 Next to its role in protecting the embryo against pathogens,  
825 *Gga-AvBD11* present in the vitelline membrane might partici-  
826 pate in the growth of the extra-embryonic yolk sac during egg  
827 incubation (roughly estimated to be at least 30  $\mu$ M based on  
828 purification yield of *Gga-AvBD11* from VM). Indeed, as the  
829 vascularized yolk sac expands during embryonic development,  
830 the vitelline membrane undergoes major ultrastructural changes  
831 to finally rupture over the embryo (41). In the present work,  
832 irrespective of the epithelial cell line being used (a chicken lung  
833 epithelial cell line (SI Appendix S23) as well as immortalized  
834 or transformed human epithelial cell lines, SI Appendix S25),  
835 we demonstrated that the full-length molecule exhibits cytotoxic  
836 effects. Interestingly, it was also shown to decrease cell invasive-  
837 ness. These data are in agreement with results obtained with the  
838 human  $\beta$ -defensin-1 (hBD-1) on oral squamous cell carcinoma  
839 (OSCC) cell lines, prostate cancer cell lines or bladder cancer cell  
840 lines (42-45). Generally, human  $\beta$ -defensins have been proposed  
841 to directly affect cancer cells by modulating their survival, pro-  
842 liferation, migration and/or invasive properties (46), with *hBD-1*  
843 being considered as a candidate tumor suppressor gene (43).  
844 Similar, but less pronounced effects were observed in the human  
845 cell lines by testing the N-ter peptide alone. The combined use  
846 of the N- and C-ter peptides was shown to affect cell viability,  
847 but to a lesser extent when compared to full-length *Gga-AvBD11*.  
848 This observation highlights the importance of the covalent link  
849 between the domains and/or the importance of the orientation of  
850 the two domains in the full-length molecule to warrant unmiti-  
851 gated activity/efficiency. *Gga-AvBD11* is essentially concentrated  
852 in the outer layer of the vitelline membrane while embryonic  
853 development, yolk sac outgrowth and expansion occur along the  
854 inner layer of the vitelline membrane, which has been reported to  
855 have growth promoting activity (47). The anti-invasive and cyto-  
856 toxic activity of *Gga-AvBD11* might thus be of major physiological  
857 importance to prevent anarchic and multidirectional cell growth  
858 of the embryo and of the yolk sac.

859 Besides these marked cytotoxic and anti-invasive effects, we  
860 did not detect any significant immunomodulatory activities of  
861 *Gga-AvBD11* and the derived peptides in human cells, although  
862 such activities have been reported for a number of other defensins  
863 (46). As stated earlier, this points to a species- or class/clade-  
864 specific role of *Gga-AvBD11* as an immunomodulatory antimicro-  
865 bial peptide.

## 866 Conclusions

867 AvBD11 is an atypical defensin which is highly conserved among  
868 birds. The 3D structure of *Gga-AvBD11* (from *Gallus gallus*) is re-  
869 ported here for the first time as the archetype of a new structural  
870 family of avian-double- $\beta$ -defensins (Av-DBD) characterized by  
871 two  $\beta$ -defensin domains packed *via* a hydrophobic cluster.

872 The conservation of *AvBD11* within bird species and its  
873 abundant and principal expression in the oviduct are pointing to  
874 important biological activities related to avian reproduction and  
875 embryonic development. Our data allowed us to confirm the role  
876 of *Gga-AvBD11* as an effector of innate immunity (most likely  
877 participating in the protection of the avian embryo) with a broad  
878 spectrum of antimicrobial activities: i) N-ter domain-dependent  
879 antibacterial activity; ii) direct antiparasitic activity against the  
880 avian protozoan *E. tenella*; and iii) antiviral activity limiting in-  
881 fluenza virus infection in avian cells –potentially by stimulating  
882 innate immunity. Moreover, from our experiments with human

883 cancer cell lines as a model for studying cell proliferation and  
884 invasiveness, we concluded that *Gga-AvBD11* might have an  
885 eminent role in driving and/or constraining the orientation and  
886 growth of embryonic and extra-embryonic cell structures in the  
887 avian egg.

888 The appearance of such a multifunctional double domain  
889 protein during evolution might have been driven by its superior  
890 effectiveness compared to a single domain molecule and/or by  
891 the necessity to acquire new functions carried only by the full-  
892 length protein. Even though the C-ter domain has no impact on  
893 the antibacterial efficacy mediated by the cationic N-ter domain  
894 (as seen for the two bacterial pathogens used here), it was shown  
895 to potentiate/increase the anti-*Eimeria*, as well as the anti-invasive  
896 biological effects. Strikingly, other activities involving interactions  
897 with eukaryotic cells, notably cytotoxic and antiviral activities in  
898 mammalian/avian cells, seem to be restricted to the full-length  
899 *Gga-AvBD11* protein.

900 In conclusion, we demonstrate here that *Gga-AvBD11* is a  
901 protein with multiple activities, a Swiss knife capable to ful-  
902 fill a number of roles that are likely essential for the proper  
903 development of the avian embryo in the egg. We believe that  
904 *Gga-AvBD11* still possesses hidden functions that merit further  
905 investigations. Studies on the contribution of *Gga-AvBD11* in  
906 the formation of the protein fibers of the outer layer of the  
907 vitelline membrane (protein-protein interactions) but also in the  
908 growth of the yolk sac during embryonic development might be  
909 of particular interest to elucidate further its physiological role(s)  
910 and underlying mechanisms.

## 911 Author contributions

912 SRG, NG and CL designed research, analyzed and integrated  
913 the data. VA and AD contributed to the design of research and  
914 overall discussion of the data. NG, AD, ST, SRG and CL wrote  
915 the manuscript. VL was involved in the mass spectrometry anal-  
916 ysis of purified *Gga-AvBD11*. VA and AD supervised chemical  
917 synthesis and folding of the domains, performed by GJ. HM and  
918 KL determined and analyzed the 3D NMR structures. NG, AS  
919 and ST designed and supervised the studies related to antibacte-  
920 rial, antiparasitic and antiviral biological activities, respectively.  
921 SI, PR and VH designed and performed the experiments related  
922 to cellular and immunomodulatory activities. All authors read the  
923 manuscript and contributed to the critical revision of the paper.

## 924 Methods

### 925 3D NMR Structures

926 Synthetic [1-40]*Gga-AvBD11*, [41-82]*Gga-AvBD11* and native *Gga-*  
927 *AvBD11* purified from vitelline membranes as previously described (6)  
928 were dissolved in H<sub>2</sub>O:D<sub>2</sub>O at a concentration of 1.25 mM, 1.40 mM and 1.08 mM,  
929 respectively. The pH was adjusted to 4.5.

930 2D <sup>1</sup>H-NOESY, 2D <sup>1</sup>H-TOCSY, sofast-HMQC (<sup>15</sup>N natural abundance) and  
931 <sup>13</sup>C-HSQC (<sup>13</sup>C natural abundance) were performed at 298K on an Avance III  
932 HD BRUKER 700 MHz spectrometer equipped with a cryoprobe. NMR data  
933 were processed using Bruker's Topspin 3.2™ and analyzed with CCPNMR  
934 (version 2.2.2) (48).

935 Structures were calculated using CNS through the automatic assignment  
936 software ARIA2 (version 2.3)(49) with NOE, hydrogen bonds and backbone  
937 dihedral angle restraints, and with three ambiguous disulfide bridges for  
938 [1-40]*Gga-AvBD11* and [41-82]*Gga-AvBD11* or two sets of three ambiguous  
939 disulfide bridges for *Gga-AvBD11*. Ten final structures were selected based  
940 on total energies and restraint violation statistics to represent each molecule,  
941 and were deposited in the Protein Data Bank under the accession codes 6QES,  
942 6QET and 6QEU, respectively.

943 Radial diffusion assay (antibacterial assays). Antibacterial assays were  
944 carried out on *Listeria monocytogenes* and *Salmonella enterica* sv. Enteri-  
945 tidis ATCC 13076 (International Center for Microbial Resources dedicated  
946 to Pathogenic Bacteria, CIRMBP, INRA, Nouzilly), as previously described  
947 for the assessment of antibacterial activities of native AvBD11 (6, 7). Pre-  
948 cultures and exponential-phase cultures were performed under agitation  
949 (180 rpm) at 37°C either in Brain Heart Infusion (BHI) or in Tryptical Soy Broth  
950 (TSB), respectively for *L. monocytogenes* and *S. enterica* Enteritidis (ATCC  
951 13076). Molten underlay medium (10 mM sodium phosphate buffer, pH 7.4,  
952 containing 0.03% TSB, 1% agarose type I low endosmosis, 0.02% Tween 20)  
953 was inoculated with exponentially growing bacteria at 3 x 10<sup>5</sup> CFU/mL and  
954 poured into a Petri dish. Wells were manually punched and filled with 5  $\mu$ L  
955

of test peptides (native *Gga*-AvBD11, N-ter and C-ter peptides, MSI-94) at different concentrations (30, 12, 4.8, 1.92, 0.768 and 0.3072  $\mu$ M) that were then allowed to diffuse within the underlay for 3h at 37°C. Underlay gel was then covered with molten overlay (10 mM sodium phosphate buffer, pH 7.4, containing 6% TSB, 1% agarose type I low endosmosis) and incubated overnight at 37°C. Antibacterial activities were revealed as clear inhibition zones surrounding the wells. Diameters of the inhibition zones were plotted against the logarithm of peptide concentrations and the linear regression equation was used to calculate the Minimal Inhibitory Concentration (12) (7).

**Antiparasitic assays.** Antiparasitic assays were performed against *Eimeria tenella* sporozoites. Sporozoites from the yellow fluorescent protein-positive (YFP) *E. tenella* strain (50) were obtained by excystation of sporulated oocysts (51). Sporozoite viability was assessed after incubation in 10 mM phosphate-buffered saline (PBS), pH7.4 with or without antimicrobial peptides (1.25 – 10  $\mu$ M) for 1 h at 41°C, and staining with aqueous Evans' blue (vol/vol). Live (green) and dead (red) parasites were counted by epifluorescence microscopy using a Zeiss Axiovert 200 microscope. Sporozoites viability is expressed as percentage of the live sporozoites incubated with PBS (considered as 100% viable). Statistical analysis was performed with Prism 5 Software (Graph-Pad) using a two-way ANOVA (Tukey Kramer Multiple Group comparison).

#### Antiviral activity assay

Cytotoxic and antiviral activities were tested using the Viral ToxGlo™ assay (Promega, USA), a luminescence-based assay measuring ATP as a surrogate for cell viability (52). Antiviral activities against an H1N1 avian influenza virus (A/Mallard/Marquenterre/Z237/83) were assayed in a chicken lung epithelial cell (CLEC213) infection model (53). Viral ToxGlo™ assay-specific 50% tissue culture infectious dose (TCID<sub>50</sub>) was determined for the viral stock according to the manufacturer's instructions. CLEC213 were seeded in 96-well plates (2.10<sup>5</sup> cells per well) and cultured in DMEM-F12 media supplemented with 7.5% fetal bovine serum (FBS), 100 U/ml penicillin and 100  $\mu$ g/ml streptomycin (Thermo Fisher Scientific, USA) at 41°C and 5% CO<sub>2</sub>. FBS was excluded from the media in subsequent treatment/infection experiments. To assess cytotoxicity, cells were washed with PBS and left untreated (controls) or treated with serial dilutions of *Gga*-AvBD11 and the N-ter or C-ter peptides (alone or in combination). To test for antiviral activity, protein/peptide dilutions were co-incubated with H1N1 at 25×TCID<sub>50</sub> (30 min at RT) and then overlaid onto the cells. At 48 h post-treatment/infection, the cells were washed and incubated with 100  $\mu$ L of ATP Detection Reagent for 20 min at RT. ATP/luminescence values were measured using a GloMax® Multi Detection System (Promega, France). Relative ATP production rates for treated and/or infected cells were calculated as fold-changes with reference to mean control values (non-treated cells) set to 1.

Dose-dependent antiviral activity of *Gga*-AvBD11 was tested by assessing H1N1 growth kinetics in non-treated/treated CLEC213. Briefly, CLEC213 were seeded in 6-well plates (8.10<sup>5</sup> cells per well) and cultured as described above. *Gga*-AvBD11 preparations (0  $\mu$ M, 0.31  $\mu$ M, 1.25  $\mu$ M or 5  $\mu$ M) diluted in culture media containing 0.05  $\mu$ g/mL TPCK-treated trypsin (Worthington Biochemical Corporation, USA) but no FBS were co-incubated with H1N1 at a multiplicity of infection (MOI) 0.01 (30 min at RT), and the mixtures were then overlaid onto the cells. At 12 h, 24 h and 48 h pi, supernatant samples (200  $\mu$ L) were collected and frozen at -80°C. Viral titers in the samples expressed as PFU/mL were determined by conventional plaque assay on Madin-Darby Canine Kidney (MDCK) cells.

1. Xiao Y, et al. (2004) A genome-wide screen identifies a single beta-defensin gene cluster in the chicken: implications for the origin and evolution of mammalian defensins. *BMC genomics* 5(1):56.
2. Kido S, Morimoto A, Kim F, & Doi Y (1992) Isolation of a novel protein from the outer layer of the vitelline membrane. *The Biochemical journal* 286 ( Pt 1):17-22.
3. Mann K (2007) The chicken egg white proteome. *Proteomics* 7(19):3558-3568.
4. Mann K (2008) Proteomic analysis of the chicken egg vitelline membrane. *Proteomics* 8(11):2322-2332.
5. Mann K, Macek B, & Olsen JV (2006) Proteomic analysis of the acid-soluble organic matrix of the chicken calcified eggshell layer. *Proteomics* 6(13):3801-3810.
6. Guyot N, et al. (2016) Proteomic analysis of egg white heparin-binding proteins: towards the identification of natural antibacterial molecules. *Scientific reports* 6:27974.
7. Herve-Grepinet V, et al. (2010) Purification and characterization of avian beta-defensin 11, an antimicrobial peptide of the hen egg. *Antimicrobial agents and chemotherapy* 54(10):4401-4409.
8. Rahman MA, Moriyama A, Iwasawa A, & Yoshizaki N (2009) Cuticle formation in quail eggs. *Zoological science* 26(7):496-499.
9. Mann K & Mann M (2013) The proteome of the calcified layer organic matrix of turkey (Meleagris gallopavo) eggshell. *Proteome science* 11(1):40.
10. Dalla Valle L, Benato F, Maistro S, Quinzani S, & Alibardi L (2012) Bioinformatic and molecular characterization of beta-defensin-like peptides isolated from the green lizard *Anolis carolinensis*. *Developmental and comparative immunology* 36(1):222-229.
11. Fry BG, et al. (2010) Novel venom proteins produced by differential domain-expression strategies in beaded lizards and gila monsters (genus *Heloderma*). *Molecular biology and evolution* 27(2):395-407.
12. van Hoek ML, et al. (2019) The Komodo dragon (*Varanus komodoensis*) genome and

Statistical differences (non-treated vs treated cells) were calculated by one-way ANOVA, unpaired T-test using GraphPad Prism v6.07 (GraphPad Software Inc., USA).

#### Invasion and MTS Cell Viability assay.

Cell invasion and viability were analyzed using Matrigel™ and MTS assays respectively, after 48 hours of incubation with various concentrations of molecules (0, 2, 4, 6 or 8  $\mu$ M). Cells used were the human non-small cell lung cancer cell line NCI-H460 and the immortalized human bronchial epithelial cell line, BEAS-2B (CRL-9609) which were obtained from the American Type Culture Collection (LGC Promochem, Molsheim, France).

Cell invasion was assessed using a modified Boyden chamber model. Two technical replicates for treated cells and three for control cells were analyzed in each independent experiment. The results were expressed as the percentage of invasive cells with reference to untreated control cell values. Results were expressed as mean  $\pm$  SEM of five independent experiments.

Cellular viability was determined by MTS assay (CellTiter 96® AQueous One Solution, Promega, Charbonnières-les-Bains, France) (SI Appendix, S25). Kruskal-Wallis test with Dunn's test was used to compare results from cells treated with different concentrations of molecules with results from control cells. Mann Whitney test was used to compare results of invasion and cytotoxicity obtained for one molecule tested at the same concentration for both assays. Statistical analyses were performed using GraphPad Prism version 6.0 for Mac OS X software.

#### Data availability

The coordinates of the ten best structures that are representative of [1-40]*Gga*-AvBD11, [41-82]*Gga*-AvBD11 and [1-82]*Gga*-AvBD11 were deposited in the Protein Data Bank, under the accession codes 6QES, 6QET and 6QEU, respectively. The chemicals' shifts were deposited in the BioMagResBank under the entries 34348, 34349 and 34350 following the same order.

#### Declarations

The authors declare that they have no competing interests.

#### Acknowledgements

This work was funded by the MUSE (Grant no. 2014-00094512) and SAPhyR-11 (Grant no. 2017-119983) project grants from the Région Centre-Val de Loire. The authors thank M. Chessé, J. Renault and J.-C. Poirier (UMR0083 BOA, INRA, University of Tours, Nouzilly, France) for their technical support in the purification of *Gga*-AvBD11. We thank G. Gabant and C. Colas (mass spectrometry platforms of UPR4301, CBM, Orléans, France and FR2708, Orléans, France, respectively) for the MS analyses of synthetic peptides. We are grateful to Ph. Roingard, J. Burlaud-Gaillard and S. Georgault (Plateforme IBSA de Microscopie Electronique, University of Tours, France) for the scanning electron microscopy analysis. We thank N. Winter, C. Schouler and A.C. Lalmanach for providing access to their bacteriological laboratories and for scientific discussions; E. Kut and J. Cournet for technical assistance in the antiparasitic and/or antiviral assays; and L. Trapp-Fragnet, D. Garrido and R. Guabiraba for providing data on viability/proliferation and NF $\kappa$ B activation in *Gga*-AvBD11-treated chicken cells (all UMR1282, ISP, INRA, University of Tours, Nouzilly, France). We also thank A. Lebrun, C. Mathé and D. Fouquet for their technical assistance in the assessment of immunomodulatory, anti-invasive and cytotoxic activities (CEPR UMR U1100, INSERM, University of Tours, Tours, France). Finally, the authors would also like to express their special gratitude to E. Kut (UMR1282, ISP, INRA, University of Tours, 37380, Nouzilly, France) for his considerable engagement in the realization of additional experiments.

13. Selsted ME & Ouellette AJ (2005) Mammalian defensins in the antimicrobial immune response. *Nature immunology* 6(6):551-557.
14. van Dijk A, Veldhuizen EJ, & Haagsma HP (2008) Avian defensins. *Veterinary immunology and immunopathology* 124(1-2):1-18.
15. Dalloul RA & Lillehoj HS (2006) Poultry coccidiosis: recent advancements in control measures and vaccine development. *Expert review of vaccines* 5(1):143-163.
16. Chang HF, Cheng HT, Chen HY, Yeung WK, & Cheng JY (2019) Doxycycline inhibits electric field-induced migration of non-small cell lung cancer (NSCLC) cells. *Scientific reports* 9(1):8094.
17. Hsia TC, et al. (2016) Cantharidin Impairs Cell Migration and Invasion of Human Lung Cancer NCI-H460 Cells via UPA and MAPK Signaling Pathways. *Anticancer research* 36(11):5989-5997.
18. Cheng Y, et al. (2015) Evolution of the avian beta-defensin and cathelicidin genes. *BMC evolutionary biology* 15:188.
19. Torres AM, et al. (2000) Defensin-like peptide-2 from platypus venom: member of a class of peptides with a distinct structural fold. *The Biochemical journal* 348 Pt 3:649-656.
20. Fox NK, Brenner SE, & Chandonia JM (2014) SCOPE: Structural Classification of Proteins-extended, integrating SCOP and ASTRAL data and classification of new structures. *Nucleic acids research* 42(Database issue):D304-309.
21. Torres AM, et al. (2014) Structure and antimicrobial activity of platypus 'intermediate' defensin-like peptide. *FEBS letters* 588(9):1821-1826.
22. Maxwell M, Undheim EAB, & Mobli M (2018) Secreted Cysteine-Rich Repeat Proteins "SCREPs": A Novel Multi-Domain Architecture. *Frontiers in pharmacology* 9:1333.
23. Arolas JL, et al. (2005) The three-dimensional structures of tick carboxypeptidase inhibitor in complex with A/B carboxypeptidases reveal a novel double-headed binding mode. *Journal*





Please review all the figures in this paginated PDF and check if the figure size is appropriate to allow reading of the text in the figure.

If readability needs to be improved then resize the figure again in 'Figure sizing' interface of Article Sizing Tool.